THE IMPORTANCE OF SEMI-MAJOR AXIS KNOWLEDGE IN THE DETERMINATION OF NEAR-CIRCULAR ORBITS

J. Russell Carpenter and Emil R. Schiesser

Primary point of contact:

Russell Carpenter
NASA/Goddard Space Flight Center
Code 572
Greenbelt, MD 20771

russell.carpenter@gsfc.nasa.gov

(301) 286-7526 (voice)
(301) 286-0369 (fax)

THE IMPORTANCE OF SEMI-MAJOR AXIS KNOWLEDGE IN THE DETERMINATION OF NEAR-CIRCULAR ORBITS

J. Russell Carpenter* and Emil R. Schiesser†

Modern orbit determination has mostly been accomplished using Cartesian coordinates. This usage has carried over in recent years to the use of GPS for satellite orbit determination. The unprecedented positioning accuracy of GPS has tended to focus attention more on the system's capability to locate the spacecraft's location at a particular epoch than on its accuracy in determination of the orbit, per se. As is well-known, the latter depends on a coordinated knowledge of position, velocity, and the correlation between their errors. Failure to determine a properly coordinated position/velocity state vector at a given epoch can lead to an epoch state that does not propagate well, and/or may not be usable for the execution of orbit adjustment maneuvers.

For the quite common case of near-circular orbits, the degree to which position and velocity estimates are properly coordinated is largely captured by the error in semi-major axis (SMA) they jointly produce. Figure 1 depicts the relationships among radius error, speed error, and their correlation which exist for a typical low altitude Earth orbit. Two familiar consequences are the relationship Figure 1 shows are the following: (1) downrange position error grows at the per orbit rate of 3π times the SMA error; (2) a velocity change imparted to the orbit will have an error of π divided by the orbit period times the SMA error. A less familiar consequence occurs in the problem of initializing the covariance matrix for a sequential orbit determination filter. An initial covariance consistent with orbital dynamics should be used if the covariance is to propagate well. Properly accounting for the SMA error of the initial state in the construction of the initial covariance accomplishes half of this objective, by specifying the partition of the covariance corresponding to down-track position and radial velocity errors. The remainder of the in-plane covariance partition may be specified in terms of the flight path angle error of the initial state. Figure 2 illustrates the effect of properly and not properly initializing a covariance. This figure was produced by propagating the covariance shown on the plot, without process noise, in a circular low Earth orbit whose period is 5828.5 seconds. The upper subplot, in which the proper relationships among position, velocity, and their correlation has been used, shows overall error growth, in terms of the standard deviations of the inertial position coordinates, of about half of the lower subplot, whose initial covariance was based on other considerations.

* Aerospace Engineer, Guidance, Navigation, and Control Center, Code 572, NASA/Goddard Space Flight Center, Greenbelt, MD.

† Senior Principal Engineer, The Boeing Company Space and Defense Systems – Houston Division, Houston, TX.

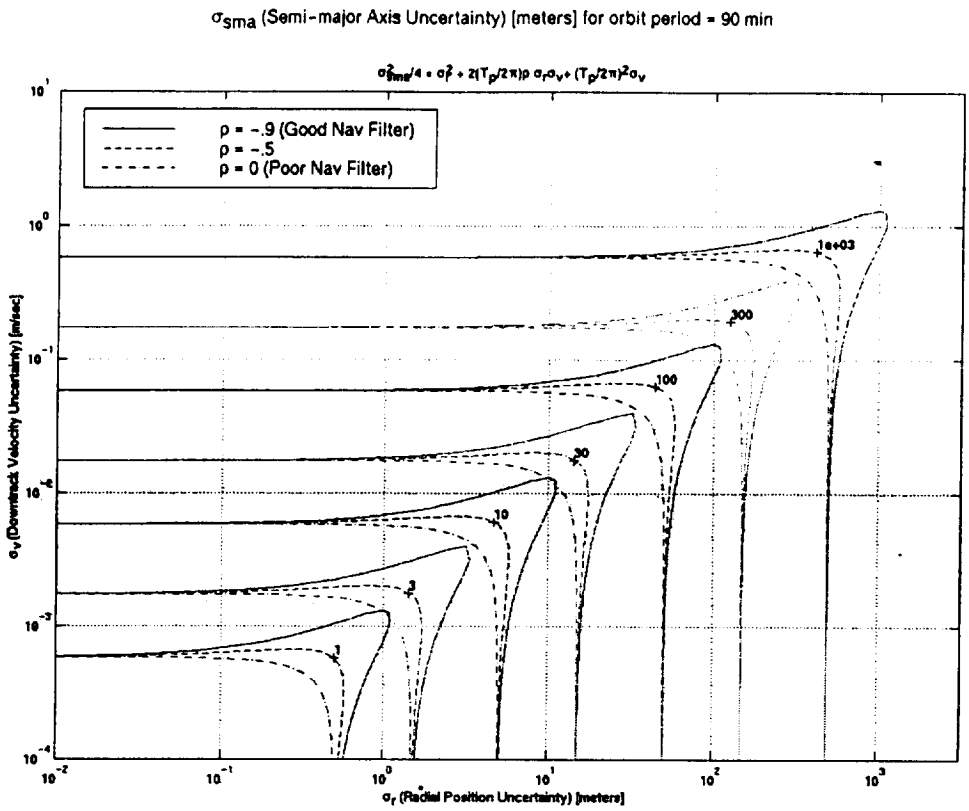

Figure 1: Semi-major axis uncertainty relationships for a typical low Earth orbit.

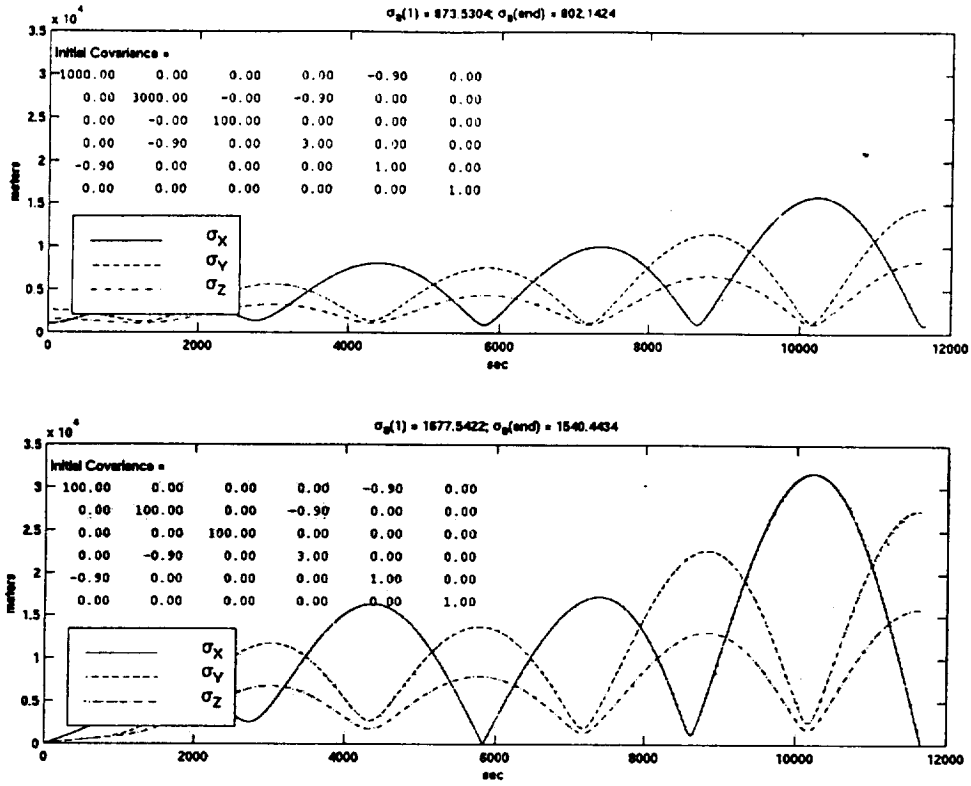

Figure 2: Comparison of covariance propagation with and without consideration of SMA and flight path angle relationships in constructing the initial covariance.

AAS 99-190

THE IMPORTANCE OF SEMI-MAJOR AXIS KNOWLEDGE IN THE DETERMINATION OF NEAR-CIRCULAR ORBITS

J. Russell Carpenter* and Emil R. Schiesser†

In recent years spacecraft designers have increasingly sought to use onboard Global Positioning System receivers for orbit determination. The superb positioning accuracy of GPS has tended to focus more attention on the system's capability to determine the spacecraft's location at a particular epoch than on accurate orbit determination, per se. The determination of orbit plane orientation and orbit shape to acceptable levels is less challenging than the determination of orbital period or semi-major axis. It is necessary to address semi-major axis mission requirements and the GPS receiver capability for orbital maneuver targeting and other operations that require trajectory prediction. Failure to determine semi-major axis accurately can result in a solution that may not be usable for targeting the execution of orbit adjustment and rendezvous maneuvers. Simple formulas, charts, and rules of thumb relating position, velocity, and semi-major axis are useful in design and analysis of GPS receivers for near circular orbit operations, including rendezvous and formation flying missions. Space Shuttle flights of a number of different GPS receivers, including a mix of unfiltered and filtered solution data and Standard and Precise Positioning Service modes, have been accomplished. These results indicate that semi-major axis is often not determined very accurately, due to a poor velocity solution and a lack of proper filtering to provide good radial and speed error correlation.

INTRODUCTION

For most people familiar with celestial mechanics, the Keplerian elements are among the most intuitive of the various parameterizations of orbital motion. However, in the modern era, orbit determination has mostly been accomplished using Cartesian coordinates. The usage of Cartesian parameters has carried over in recent years to the use of the Global Positioning System (GPS) for satellite orbit determination. The unprecedented positioning accuracy of GPS has tended to focus attention more on the system's capability to locate the spacecraft's location at a particular epoch than on its accuracy in determination of the orbit, per se. As is well known, the latter depends on a coordinated knowledge of position, velocity, and the correlation between their errors. Failure to determine a properly coordinated position/velocity state vector at a given epoch can lead to an epoch state that does not propagate well, and/or may not be usable for the execution of orbit adjustment maneuvers. With a few elementary equations from celestial mechanics, the authors and their colleagues have developed a handy set of back-of-the-envelope guidelines and charts which have been found useful in analyzing and designing orbit determination systems for near-circular orbits. It is hoped that dissemination of these rules of thumb will help to refocus attention, especially

* Aerospace Engineer, Guidance, Navigation, and Control Center, Code 572, NASA Goddard Space Flight Center, Greenbelt, MD 20771.

† Specialist Engineering, The Boeing Company Space and Defense Systems - Houston Division, Houston, TX 77058.

among the rapidly expanding community of GPS orbit determination users, on the importance of determining the whole orbit, not just the satellite's position.

Coordination of Position and Velocity

Many aspects of the degree to which position and velocity estimates are properly coordinated are captured by the error in semi-major axis (SMA) their own errors jointly produce. These errors in position and velocity can be considered to be knowledge errors in the current orbit, or maneuver execution errors created in trying to achieve an orbit change. Kepler discovered that for an ideal orbit, the square of the period is proportional to the cube of the semi-major axis. Thus, the magnitude and degree of proper coordination of position and velocity knowledge errors, as measured by the error in SMA, is equivalently to a statement of the knowledge error in orbit period. Letting T_p denote the period, and a denote the SMA, Kepler's law may be written[1]

$$T_p = 2\pi\sqrt{\frac{a^3}{\mu}}, \tag{1}$$

where $\mu = GM$, the product of the gravitational constant, G, and the planetary mass, M. Taking variations on Eq. (1), it is easy to show[2] that a variation, δa, in the nominal SMA, leads to a variation in period, δT_p, given by

$$\delta T_p = 3\pi\sqrt{\frac{a}{\mu}}\delta a. \tag{2}$$

Based on the principle of conservation of energy, it can also be shown[1] that the sum of kinetic and potential energy must be a constant, $-\mu/(2a)$. Thus, SMA knowledge is also an indication of knowledge of the orbit's energy. Letting v denote the velocity magnitude and r denote the position magnitude, the energy integral may be written

$$\frac{1}{a} = \frac{2}{r} - \frac{v^2}{\mu}, \tag{3}$$

from which the following variational equation is apparent:

$$\frac{1}{a^2}\delta a = \frac{2}{r^2}\delta r + \frac{2v}{\mu}\delta v. \tag{4}$$

One drawback to Eq. (3) is that it is based on Kepler's two-body potential. For real orbits, the J_2 oblateness term alone causes variations on the order of a few kilometers per orbit. For this reason, so-called mean element sets are often useful. However, this paper is primarily concerned with the effects and analysis of variations in the osculating semi-major axis, which is derived from the instantaneous position and velocity. A useful indicator of the coordination of the directions of the position and velocity vectors is the flight-path angle, γ, which is the complement of the angle between the velocity vector, $\boldsymbol{v}$, and the position vector, $\boldsymbol{r}$:

$$\|\boldsymbol{r}\|\|\boldsymbol{v}\|\sin\gamma = \boldsymbol{r}\cdot\boldsymbol{v}. \tag{5}$$

Many orbits of practical interest, such as low Earth orbits (LEO) and geosynchronous Earth orbits (GEO), are nearly circular. In such orbits, one can assume that the velocity is approximately the circular orbit velocity $(\mu/r)^{1/2}$, and that $a \approx r$. With these assumptions, Eq. (4) simplifies to Eq. (6):

$$\delta a = 2\delta r + \frac{2r}{v}\delta v \tag{6}$$

To simplify Eq. (5), one may also assume that $\sin(\gamma) \approx \gamma \approx 0$. It is also useful to consider an orthogonal set of perturbations in the radial, along-track, and cross-track directions, δu, δs, and δw, and their time derivatives, denoted by overdots. In terms of the notation used above, $\delta u = \delta r$, and for near-circular orbits, $\delta \dot{s} \approx \delta v$. Then, Eq. (5) simplifies as follows:

$$\begin{aligned} \delta\gamma &\approx [r, 0, 0]\cdot[\delta\dot{u}, \delta\dot{s}, \delta\dot{w}] + [0, v, 0]\cdot[\delta u, \delta s, \delta w] \\ &= r\delta\dot{u} + v\delta s \end{aligned} \tag{7}$$

Proper coordination of position and velocity for near-circular orbits means that in-plane perturbations in position and velocity must balance one another in order to preserve the semi-major axis (i.e. period, energy) of the nominal or targeted orbit. Proper coordination also preserves the approximately zero flight-path angle (i.e. zero eccentricity) of the orbit. Thus, Eq. (6) tells one that if δa is held to zero to preserve the nominal or targeted SMA, a change in (down-track) velocity must be balanced by a radial change in position:

$$\delta u = -\frac{r}{v}\delta\dot{s}. \tag{8}$$

For LEO cases, the ratio r/v is approximately 1000. Thus a 1 meter per second down-track velocity perturbation must be balanced by a −1000 meter radial position perturbation if SMA is to be maintained. Also, Eq. (7) tells one that if $\delta\gamma$ is held to zero to preserve the nominally zero flight-path angle, then a change in along-track position, δs, must be compensated by a change in radial velocity:

$$\delta\dot{u} = -\frac{v}{r}\delta s. \tag{9}$$

The same ratio of approximately 1000 to 1 appears for LEO cases, so that a 1 meter per second perturbation to radial velocity must be balance by a −1000 meter change in down-track position, if near-zero flight-path angle is to be maintained. The authors have found Eqs. (8) and (9), especially in the form of the two "1000 to 1" rules for LEO cases, to be useful and easy to remember.

Problems Caused by Poor Semi-Major Axis Knowledge

Down-track error growth. A familiar example of problems caused by inaccurate SMA knowledge is down-track position error growth. This problem arises because any SMA error will produce a period error (Eq. (2)); thus the satellite will complete more or less than one

actual revolution during its nominal period. For near-circular orbits, the resulting along-track error for one revolution is

$$\delta s = -v\delta T_p, \tag{10}$$

where the negative sign convention recognizes that if the actual period is less than nominal, the satellite ends up farther along in its orbit than nominal, which is taken to be a positive along-track error. If one substitutes Eq. (2) into Eq. (10), and takes the velocity to be the circular orbit velocity, then one finds that

$$\delta s = -3\pi\delta a, \tag{11}$$

which is a common rule of thumb for down-track error growth[2].

Manuever execution errors. In the case of an instantaneous maneuver, there is no position change, so Eq. (8) states that unless any total velocity error (knowledge plus maneuver execution error) is balanced by a corresponding radial position knowledge error, there will inevitably be a semi-major axis error. Correspondingly, if position and velocity knowledge errors are properly coordinated, then the SMA error resulting from an instantaneous maneuver will be solely due to maneuver execution errors. Thus, for a given maneuver execution error magnitude, the error in the resulting SMA is minimized if position and velocity are properly coordinated.

Covariance matrix propagation. A less familiar example occurs in the problem of initializing the covariance matrix for a sequential orbit determination filter that uses Cartesian coordinates. One of the advantages often cited in favor of sequential filtering is that the entire state need not be fully observed at any given epoch, because observability of the in-plane projections of the state occurs over time due to correlations inherent in the dynamics of orbital motion. However, an initial covariance consistent with the parameters of the orbit must also be used if the covariance is to propagate well during the period in which insufficient measurements to fully observe the state are available.

For many orbits, the two simple rules of thumb given by Eqs. (8) and (9) may be used to specify the in-plane diagonal elements of an appropriate initial covariance matrix (a more detailed discussion of semi-major axis uncertainty and correlations among the covariance matrix elements is given in the subsequent section). One should use Eq. (8) to specify the partition of the covariance corresponding to down-track position and radial velocity errors that are consistent with the SMA error of the initial state. For near-circular orbits, the remainder of the in-plane covariance partition may be specified using Eq. (9) to specify radial velocity and down-track position errors that are consistent with the flight path angle error of the initial state.

Figure 1 illustrates the effect of properly and not properly initializing the covariance. This figure was produced by propagating the initial covariance shown on the plot, without process noise, in a circular low Earth orbit whose period is 5828.5 seconds. The initial and final values of the SMA uncertainty (computed using Eq. (15) shown in the next section) are given at

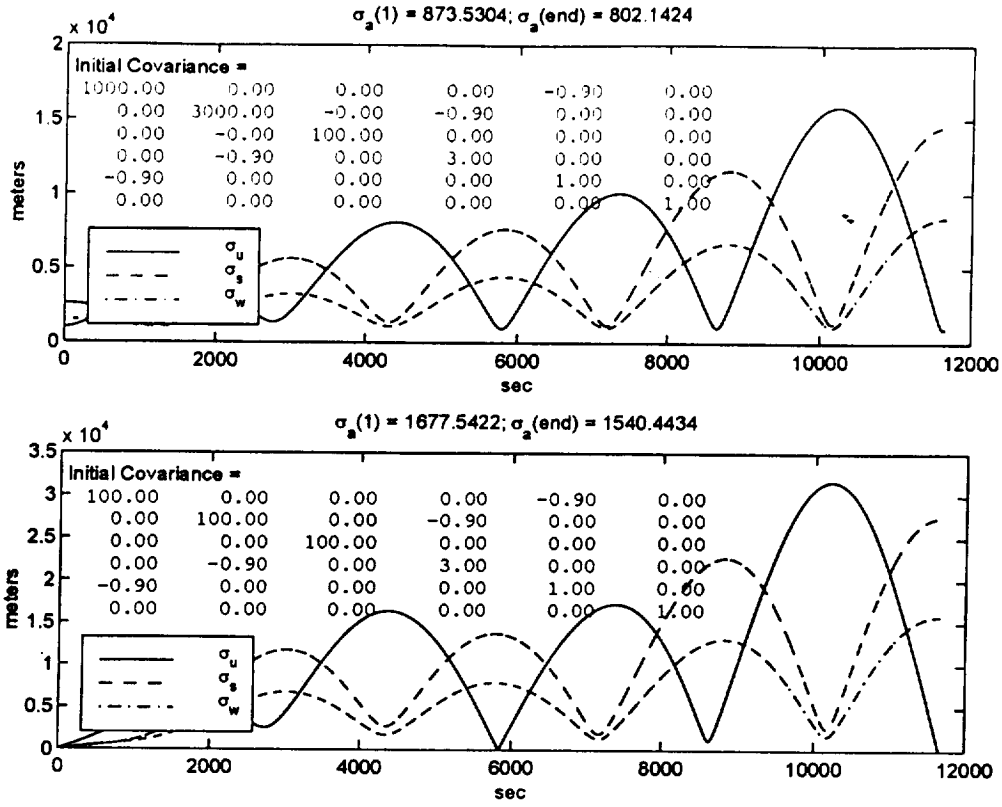

Figure 1: Comparison of covariance propagation with and without consideration of SMA and flight-path angle relationships in the construction of the initial covariance.

the top of each plot. The upper subplot, in which the proper relationships among position, velocity, and their correlation have been used, shows overall error growth, in terms of the standard deviations of the inertial position coordinates, of about half of the lower subplot, whose initial covariance was based on arbitrary considerations. Note how close the radial position error comes to zero just before 6000 seconds in the lower subplot; this is a warning sign that one of the eigenvalues of the covariance matrix may be about to become non-positive.

SIMPLE FORMULAS FOR SEMI-MAJOR AXIS UNCERTAINTY

This section illustrates some simple formulas and charts that relate the statistical variance of the Cartesian states to the semi-major variance. Modification of these formulas for relative navigation applications is also discussed.

Absolute State Semi-major Axis

One may regard semi-major axis as a non-linear function of the Cartesian state vector $x = [r^T, v^T]$. Then, a first order approximation that relates changes in the state away from a nominal value (denoted by the subscript o) to changes in the SMA is given by

$$a - a_o \approx \left.\frac{\partial a}{\partial x}\right|_{x=x_o} (x - x_o). \tag{12}$$

Letting

$$A(x_o) = \left.\frac{\partial a}{\partial x}\right|_{x=x_o} = 2a^2 \left[\frac{r^T}{\|r\|^3}, \frac{v^T}{\mu}\right]_{x=x_o}, \tag{13}$$

where the partial derivative has been evaluated assuming a two-body potential, one may write the error variance of the SMA in terms of the state error covariance using Eqs. (12) and (13) as follows:

$$\begin{aligned} \mathrm{E}\left[(a - a_o)^2\right] &= \mathrm{E}\left[A(x_o)(x - x_o)(x - x_o)^T A(x_o)^T\right] \\ \sigma_a^2(x_o) &= A(x_o) P_x A(x_o)^T \end{aligned} \tag{14}$$

In deriving Eq. (14), the symbol "E" denotes the expectation operator, and P_x is the state error covariance matrix. In Reference 2 one finds the following simplification of Eq. (14), valid for near-circular orbits:

$$\sigma_a = 2\sqrt{\sigma_u^2 + 2\left(\frac{T_p}{2\pi}\right)\rho_{us}\sigma_u\sigma_s + \left(\frac{T_p}{2\pi}\right)^2 \sigma_s^2}. \tag{15}$$

In Eq. (15), ρ_{us} denotes the correlation coefficient between radial position error and down-track velocity error, and σ_u and σ_s denote the radial position error and down-track velocity error standard deviations, respectively.

The authors have found Eq. (15) to be a useful design and analysis aid, especially in graphical form. Also, either Eq. (14) or Eq. (15) is useful as a "figure of merit" for orbit determination filters. Figure 2 shows one means of graphically representing Eq. (15) for LEO scenarios. Figure 2 depicts several families of relationships among the principal contributors to SMA uncertainty for a LEO mission. Each family of curves illustrates a subset of the range of radial position and down-track velocity errors that generate the **same** SMA error, from 0.1 meter to 1000 meters.

Along the main diagonal of the chart, the families split based on the value of the correlation coefficient. The correlation coefficient captures the deterministic relationship implied among the radial position and down-track velocity errors by Eq. (8). To the extent that these errors are properly coordinated, a given level of knowledge about either one implies some degree of knowledge about the other. The coefficient is negative because of the negative relationship stated by Eq. (8). The region of the plot in which the families split corresponds to a "sweet spot" of proper coordination among position and velocity.

At one extreme, radial position and down-track velocity errors are completely uncorrelated ($\rho = 0$), and the SMA error is bounded below by the lower of its corresponding radial position and down-track velocity errors. For example, no matter how good position knowledge gets, SMA knowledge will be no better than about 100 meters if down-track velocity knowledge cannot be improved beyond about 0.05 meters per second. However, if radial position and down-track velocity errors are properly coordinated (via Eq. (8)), the SMA knowledge can be dramatically improved, because a corresponding increase in the correlation among radial position and down-track velocity errors is possible. For example, using the "1000 to 1" rule of Eq. (8), a radial position error of 100 meters should correspond to a down-track velocity error of about –.1 meters per second. As Figure 2 shows, this combination could correspond to an SMA error of about 100 meters if the correlation coefficient is –.9, but would only correspond to an SMA error of just under 300 meters if the correlation coefficient is near zero. A coefficient near the value one would expect if Eq. (8) were nearly exactly satisfied (~ –0.99) would give an SMA error on the order of 30 meters. In the limit, the coefficient reaches –1, the horizontal and vertical branches on the plot disappear, the random variables become simple deterministic variables, and the linear relationship of Eq. (8) is depicted as a straight line from lower left to upper right.

Relative State Semi-major Axis

For some missions involving one or more vehicles, such as rendezvous and docking or for-

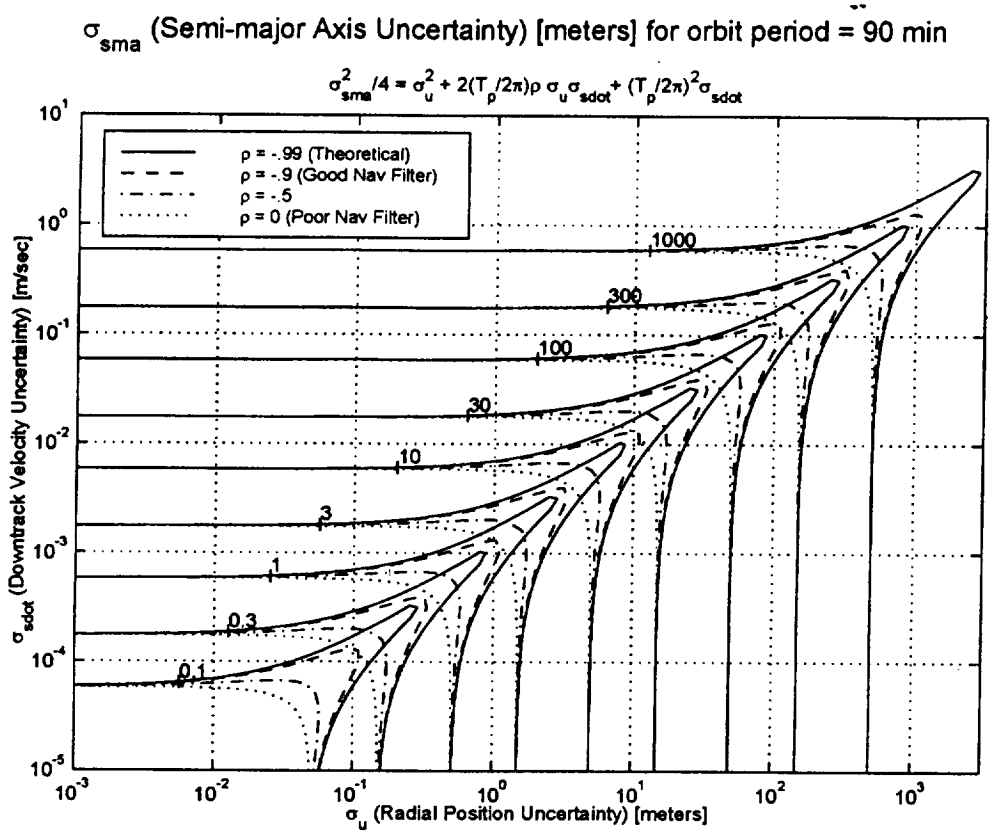

Figure 2: Semi-major axis uncertainty relationships for a typical low Earth orbit.

mation flying missions, a parameter of interest is the relative SMA, i.e. the difference in SMA between pairs of vehicles. To illustrate, suppose a "chaser" spacecraft is attempting a rendezvous with a target spacecraft. Denoting the chaser SMA by a_c, and the target SMA by a_t, the relative SMA is

$$a_{rel} = a_c - a_t. \tag{16}$$

Since a_c is a function of the chaser state x_c and a_t is a function of the target state x_t, in deriving the uncertainty of the relative SMA it is useful to define an augmented state consisting of both the chaser and target states: $x^T = [x_c^T \; x_t^T]$. Then, as in Eq. (12), a perturbation in the nominal relative SMA may be approximated by

$$a_{rel} - a_{rel_o} \approx \left.\frac{\partial a_{rel}}{\partial x}\right|_{x=x_o} (x - x_o). \tag{17}$$

Using the notation of Eq. (13), the partial derivative is evaluated as follows:

$$\left.\frac{\partial a_{rel}}{\partial x}\right|_{x=x_o} = \left[2a_c{}^2\left[\frac{r_c^{\mathsf{T}}}{\|r_c\|^3}, \frac{v_c^{\mathsf{T}}}{\mu}\right], -2a_t{}^2\left[\frac{r_t^{\mathsf{T}}}{\|r_t\|^3}, \frac{v_t^{\mathsf{T}}}{\mu}\right]\right]_{x=x_o} \tag{18}$$

$$A(x_o) = \left[A_c(x_o), -A_t(x_o)\right]$$

The covariance of the chaser/target state, P_x, may be partitioned into chaser-only and target-only covariances (P_c and P_t), and their cross-covariance matrices (P_{ct}):

$$P_x = \begin{bmatrix} P_c & P_{ct} \\ P_{ct}^{\mathsf{T}} & P_t \end{bmatrix}. \tag{19}$$

Using Eqs. (18) and (19) in Eq. (14) results in the following:

$$\begin{aligned} \sigma_{a_{rel}}^2 &= \left[A_c(x_o), -A_t(x_o)\right]\begin{bmatrix} P_c & P_{ct} \\ P_{ct}^{\mathsf{T}} & P_t \end{bmatrix}\left[A_c(x_o), -A_t(x_o)\right]^{\mathsf{T}} \\ &= A_c P_c A_c^{\mathsf{T}} + A_t P_t A_t^{\mathsf{T}} - A_c P_{ct} A_t^{\mathsf{T}} - \left(A_c P_{ct} A_t^{\mathsf{T}}\right)^{\mathsf{T}} \end{aligned} \tag{20}$$

FLIGHT PERFORMANCE SURVEY

Space Shuttle flights of a number of different GPS receivers, including a mix of unfiltered and filtered solution data and Standard and Precise Positioning Service modes, have been accomplished. Both absolute state and relative state performance have been evaluated. Particular interest has been given to the semi-major axis performance of the GPS receivers and any associated filtering algorithms, to determine if the GPS has the potential to replace or augment existing navigation sensors.

Absolute State Flight Performance

Absolute state flight data results are shown in Table 1, and in Figure 3, the flight data are overlayed on a copy of Figure 2. The data used in constructing these tables was extracted from Refs. 3-6, and from various internal documents. In some cases, either velocity or SMA data were not available. In general, the flight data indicate that semi-major axis is often not determined very accurately, typically due to a poor velocity solution and/or a lack of proper filtering to provide good radial and speed error correlation. Note that the flight data are all from LEO missions, but have periods varying by a few minutes from the nominal period of 90 minutes used to construct the figure.

It is interesting to observe that nearly all the flight data lie above the diagonal region in Figure 3 previously described as the "sweet spot" for proper coordination of position and velocity. This indicates that GPS is generally determining position too accurately in comparison to its velocity accuracy for it to produce SMA accuracy comparable to its position accuracy. Cases J and B happen to lie in the "sweet spot," but Table 1 reveals that their SMA accuracy corresponds to a near-zero correlation coefficient. Thus, these cases are not taking advantage of the potential improvement in SMA to the order of 10-30 m they could otherwise achieve.

To establish performance, the flight data are compared to best estimated trajectories (BETs), generated with various procedures. Most of the BET procedures have been verified to be accurate to about 30 meters RMS in position and a few hundredths of a meter per second RMS in velocity[7]. The Post-flight Attitude and Trajectory History (PATH) BET is probably less accurate in position, but more accurate in velocity, than the Wide Area Differential GPS (WADGPS) BET. (The PATH accuracy is specified to be on the order of 200 meters in position and 0.2 m/s in velocity RMS in the worst axis, but it is generally believed to be much better.) In some cases, filtered position data from an independent, PPS-capable GPS receiver

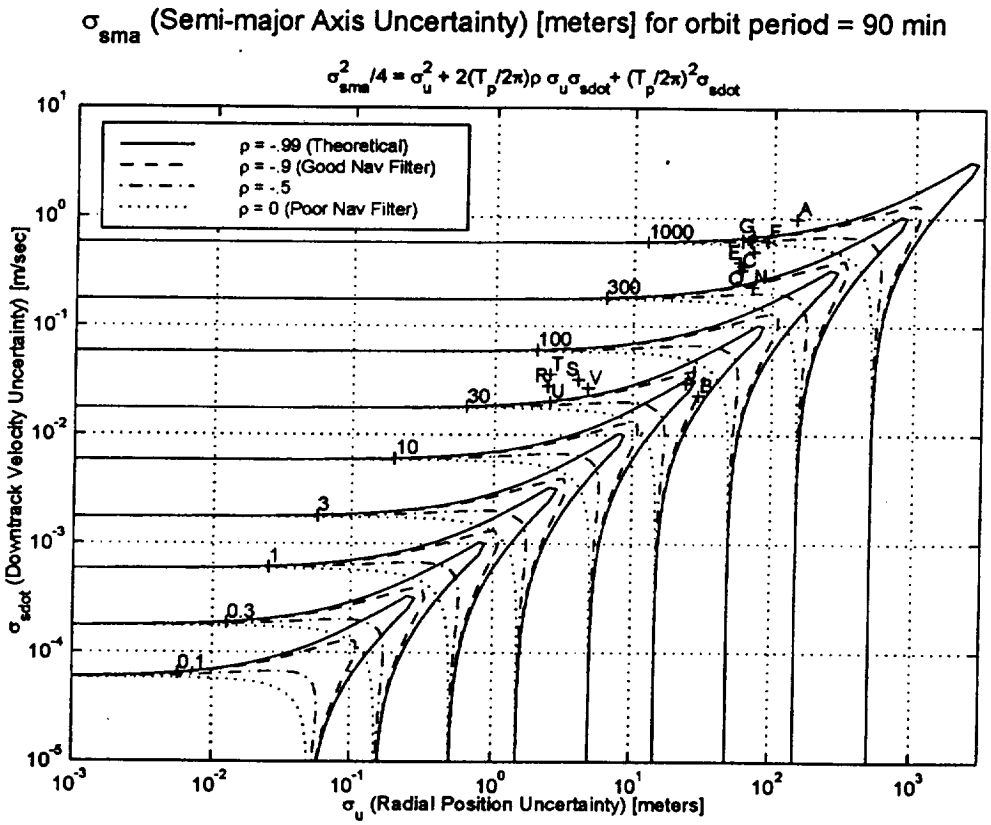

Figure 3: Semi-major axis uncertainty flight data results overlayed on SMA uncertainty relationships for a typical low Earth orbit.

was used as the BET. These BETs are believed to be slightly more accurate in position than the WADGPS BET, and comparable to the PATH BET in velocity.

Table 1
ABSOLUTE STATE GPS ORBITAL FLIGHT PERFORMACE SURVEY

Case	Flight	Receivers	Flight Phase	Solution	No. of Chan	Rec. Det./Filt.	Measure-ment	Position, m				Velocity, m/s				SMA, m	Comparison
								Radial	In-track	X-track	RSS	Radial	In-track	X-track	RSS		
A	STS-51	TANS Quadrex	Orbit	Rec	6	d	C/A	145.5	97	97	200	1.455	0.97	0.97	2	1000	Filtered
B	STS-69	RI/Collins 3M	Orbit	RGPS	5 (1 rov)	f (gd)	C/A	30	20	20	41.2	0.034	0.023	0.023	0.047	100	WADGPS BET
C	STS-69	RI/Collins 3M	Orbit	Rec	5 (1 rov)	d	C/A	60	40	40	82.5	0.492	0.328	0.328	0.676	700	WADGPS BET
D	STS-69	TurboRogue	Orbit	Rec	8	d	C/A	36	18	48	63	-	-	-	-	-	Least square fit to T.Rogue pos
E	STS-80	TANS Quadrex	Orbit	Rec	6	d	C/A	58.2	38.8	38.8	80	0.582	0.388	0.388	0.8	803.3	WADGPS BET
F	STS-80	Laben Tensor	Orbit	Rec	9	d	C/A	91	60.6	60.6	125	0.91	0.606	0.606	1.25	1255.1	WADGPS BET
G	STS-80	TANS Quadrex	Orbit	Rec	6	d	C/A	72.8	48.5	48.5	100	1.019	0.679	0.679	1.4	1347.5	WADGPS BET
H	STS-80	Laben Tensor	Orbit	Rec	9	d	C/A	72.8	48.5	48.5	100	0.728	0.485	0.485	1	1004.1	WADGPS BET
I	STS-81	RI/Collins MAGR	Orbit	Rec	5 (1 rov)	f	C/A	25.1	16.7	16.7	34.4	-	17.678	-	18	-	TDRS Vectors
J	STS-84	RI/Collins MAGR	Orbit	Rec	5 (1 rov)	f	C/A	24.4	18.3	53.3	61.4	0.046	0.03	0.03	0.063	73.2	PATH BET
K	STS-84	HI-EGI/GEM-III	Orbit	Rec	5 (1 rov)	f	C/A	40	30	30	58.3	0.5	0.4	0.4	0.755	-	BET
L	STS-84	HI-EGI/GEM-III	Orbit	Blended	5 (1 rov)	f	C/A	70	50	50	99.5	0.5	0.5	0.7	0.995	-	WADGPS BET
M	STS-84	HI-EGI/GEM-III	Orbit	Rec	5 (1 rov)	f	C/A	75	40	35	91.9	0.5	0.3	0.3	0.656	-	WADGPS BET
N	STS-84	HI-EGI/GEM-III	Orbit	Rec	5 (1 rov)	f	C/A	72	270	38	282	0.62	0.23	0.18	0.685	372	WADGPS BET
O	STS-84	HI-EGI/GEM-III	MECO	Rec	5 (1 rov)	f	C/A	37.1	24.7	24.7	51	1.601	1.067	1.067	2.2	-	Ascent BET
P	STS-86	HI-SIGI/GEM-III	MECO	Rec	5 (1 rov)	f	Y	88	58.7	58.7	121	0.116	0.078	0.078	0.16	-	Ascent BET
Q	STS-86	Litton-EGI/GEM-III	Orbit	Rec	5 (1 rov)	f	C/A	61.5	27.6	23.4	71.4	0.547	0.359	0.288	0.715	564.3	BET using GEM III position
R	STS-89	HI-SIGI/GEM-III	Orbit	Rec	5 (1 rov)	f	Y	2.4	1.2	1.2	3	0.026	0.028	0.016	0.042	50	Least square fit to receiver pos.
S	STS-89	HI-SIGI/GEM-III	Orbit	Rec	5 (1 rov)	f	Y	4	3.1	2.8	5.8	0.033	0.032	0.017	0.048	57.7	BET using MAGR pos
T	STS-91	HI-SIGI/GEM-III	Orbit	Rec	5 (1 rov)	f	Y	2.5	3.6	1.4	4.6	0.03	0.036	0.016	0.05	62.9	BET using GEM III pos (24 hr arc)
U	STS-91	HI-SIGI/GEM-III	Orbit	Rec	5 (1 rov)	f	Y	2.5	1.4	1.3	3.2	0.02	0.02	0.02	0.03	35	BET using GEM III pos (40 mn)
V	STS-91	HI-SIGI/GEM-III	Orbit	Rec	5(1 rov)	f	Y	4.7	4.3	15.4	16.6	0.029	0.027	0.016	0.043	47.3	BET using MAGR pos (12 hrs)
	Overall C/A Performance					d	C/A	65.1	42.4	47.4	91	0.746	0.497	0.497	1.025	1022	
						f	C/A	52.6	30.4	35.2	70.2	0.452	0.303	0.316	0.63	336.5	
	Overall Y Code Performance					f	Y	3.2	2.7	2.2	4.7	0.027	0.029	0.017	0.043	50.6	

Notes:

- No. of Chan.: number of GPS receiver channels; (1 rov) indicates a roving channel is used for L2 tracking and GPS satellite acquisition (data are obtained from up to four GPS satellites at a time).
- The "Rec." column identifies filtered ("f") vs. deterministic ("d") GPS receiver/processor solution output, and "f(gd)" indicates filtering performed on the ground, post-flight.
- The "Comparison" column identifies the standard with which the GPS results were compared
  - WADGPS BET is a Wide-Area Differential GPS Best Estimated Trajectory in which ground-based GPS receiver data are used to remove Selective Availability and other error effects from onboard GPS receiver measurements[7].
  - TDRS indicates that four Mission Control Center ground navigation batch solution state vectors, derived from Tracking and Data Relay Satellite S-band data, were compared with GPS solutions; PATH BET is a forward/backward batch solution using similar data.
- The last (STS-91) record reflects a 15 m crosstrack difference between the GEM-III and MAGR-based BET which was not included in the overall Y-code performance figure.
- The"Sol" column identifies the type of solution evaluated: "Rec" is a receiver solution, "RGPS" is a solution for the absolute state from the RGPS filter[3], and "Blended" is from the SIGI GPS/INS blended solution.
- Other acronym definitions: TANS: Trimble Advanced Navigation System; MAGR: Miniature Airborne GPS Receiver; RI: Rockwell International (now Boeing); HI: Honeywell International; EGI: Embedded GPS/INS; SIGI: Space Integrated GPS/INS; MECO: Main Engine Cut-Off; C/A: Coarse/Acquisition; X-track: cross-track; RSS: root sum squared

Table 2
RGPS FLIGHT EXPERIMENTS PERFORMANCE SURVEY

Flight	Receivers		Rel. Motion	No. Comm. GPS SVs	Measure-ment	Rel. Position, m				Rel. Velocity, m/s				Rel. SMA, m	Comparison
	Chaser	Target				Radial	In-track	X-track	RSS	Radial	In-track	X-track	RSS		
STS-69	Collins 3M	Turborogue	Sep.	<=3	C/A,C/A	80.0	40.0	50.0	102.5	-	-	-	-	200	Diff. of 2 WADGPS BETs
STS-80	TANS Quadrex	Laben Tensor	Rendez.	<=6	C/A,C/A	7.6	3.9	2.9	9.0	0.089	0.061	0.042	0.120	110	Laser BET

Relative State Flight Performance

NASA has jointly performed two relative GPS (RGPS) navigation flight experiments with the European Space Agency (ESA)[3-6]. During these experiments, a near-realtime relative GPS Kalman filter processed data measurement data from GPS receivers aboard the Space Shuttle and a free flying satellite deployed and retrieved by the Shuttle. This filter was designed to estimate common biases affecting GPS receivers aboard two co-orbiting spacecraft tracking the same GPS satellites. When measurements from at least four common satellites are available, it is expected that differential GPS accuracy could be obtained. Table 2 summarizes the performance from these missions. It should be noted that an ESA-developed Kalman filter processed the STS-80 data postflight and achieved results similar to, or slightly better than, the STS-80 results quoted in Table 2.

These data may be compared with Table 3, which shows typical performance of the existing Shuttle rendezvous navigation system. The existing system consists of a rendezvous radar providing range, range-rate, azimuth and elevation measurements to an extended Kalman filter that also utilizes acceleration data from an inertial measurement

Table 3
PERFORMANCE OF EXISTING SHUTTLE RENDEZVOUS NAVIGATION SYSTEM ON STS-80

Position (m)				Velocity (m/s)				SMA (m)
Radial	In-track	X-track	RSS	Radial	In-track	X-track	RSS	
15.1	3.6	1.7	15.6	0.023	0.015	0.008	0.029	49.4

unit. The data were derived by comparison of the downlinked Shuttle relative navigation data to a laser-based best estimated trajectory (BET) produced after the flight. In particular note that although the relative GPS position accuracy of Table 2 is somewhat better than the relative position accuracy of the Shuttle's existing system shown in Table 3, the SMA accuracy is more than twice as inaccurate. The performance difference is primarily due to poorer relative velocity estimates from the RGPS filter, but also due to poorer correlation among position and velocity errors.

Another approach to GPS relative navigation is to directly difference the solutions from two GPS receivers, rather than process the measurement data from both receivers in a

Table 4
STATE VECTOR DIFFERENCING PERFORMANCE DURING STS-80 RGPS FLIGHT EXPERIMENT

Sol	Measure-	Position (m)				Velocity (m/s)				SMA (m)
Det/Filt	ment	Radial	In-track	X-track	RSS	Radial	In-track	X-track	RSS	
d,d	C/A, C/A	138.0	51.7	57.0	158.1	1.699	0.949	0.550	2.022	1706.0

single Kalman filter as described above. Such an approach is obviously much simpler, but does not remove the common error sources. As Table 4 shows, the state vector dif-

ferencing performance data from STS-80 show significantly worse performance than the filtered results Table 2 presents.

However, if the receivers can be operated under the Precise Positioning Service (PPS), with dual-frequency P/Y-code measurements, most errors larger than a few meters are removed. Under such circumstances, it could be feasible to perform GPS relative navigation using state vector differencing. Although no known flight experiments have been conducted using the PPS, Table 5 shows an attempt at bounding the performance of such

Table 5
STATE VECTOR DIFFERENCING PERFORMANCE SURVEY
DERIVED FROM TABLE 1 FLIGHT DATA

Sol	Measure-	Position (m)				Velocity (m/s)				SMA (m)
Det/Filt	ment	Radial	In-track	X-track	RSS	Radial	In-track	X-track	RSS	
d, d	C/A, C/A	92.1	60.0	67.0	128.7	1.055	0.703	0.703	1.450	1445.3
d, f	C/A, C/A	83.7	52.2	59.1	115.0	0.872	0.582	0.589	1.203	1076.0
d, f	C/A, Y	65.2	42.5	47.5	91.2	0.746	0.498	0.498	1.026	1023.3
f, f	C/A, C/A	74.3	43.0	49.8	99.3	0.639	0.429	0.448	0.891	475.9
f, f	C/A, Y	52.7	30.6	35.3	70.4	0.453	0.305	0.317	0.631	340.3
f, f	Y, Y	4.6	3.8	3.0	6.7	0.039	0.041	0.024	0.061	71.5

a configuration, using the absolute state performance data from Table 1. In Table 5, the values were obtained by computing the root sum squares of the overall absolute state performance figures at the bottom of Table 1, assuming that the errors in the two receivers are uncorrelated (i.e. $P_{ct} = 0$). Table 5 contains figures for both absolute states computed deterministically by the receivers, and absolute states resulting from onboard orbit determination filters (denoted "d" and "f," respectively, in the first column).

Clearly, although filtering the data helps significantly, state vector differencing, even if one of the two receivers is P/Y-code capable, is not competitive with either the RGPS filtering approach or the existing Shuttle rendezvous system capabilities (viz. Tables 2 and 3). However, the data representing filtered absolute state differences using P/Y-code measurements, shown in the last row of Table 5, are superior to the RGPS filter performance (Table 2), and are close to comparable with the existing Shuttle rendezvous system (Table 3). Note that flight data results are not known to be available for deterministic P/Y-code absolute state differences, nor are flight results from an RGPS-type filter using P/Y-code measurements.

Also note that none of the flight data results presented utilize carrier phase data, which is commonly used in static surveying applications to achieve centimeter-level relative positioning. Carrier phase measurements are analogous to a very accurate pseudo-range measurement. Based on the flight data results presented above, it may be hypothesized that improvements in position knowledge such as might be achieved with carrier phase processing cannot necessarily be counted upon to significantly improve semi-major axis knowledge. Based on Figure 2, one might argue that even were position known to better than 1 centimeter, if velocity knowledge on the order of 0.1-1 millimeters per second

were not also achieved (along with good correlation among position and velocity errors), then SMA knowledge could not be improved over existing levels of performance.

CONCLUSION

This paper has argued that achieving good semi-major axis knowledge should be an important consideration in orbit determination applications. Nevertheless, flight data results from a number of Space Shuttle GPS experiments, employing a number of different GPS receivers and navigation filtering approaches, indicate that semi-major axis is often not determined very accurately in space applications of GPS. It has been argued, and the flight data generally support, that the lack of good semi-major axis knowledge is primarily due to a poor velocity solution and a lack of proper filtering to provide good radial and speed error correlation. Use of carrier phase data does not appear to improve this situation, unless it is accompanied by proper filtering that accounts for the orbital dynamics and the correlations they impose on the dynamics of this problem. It is quite possible that the existence of this issue can be attributed to a lack of awareness on the part of the GPS community about the importance of semi-major axis knowledge. Several simple equations, rules of thumb, and charts concerning the semi-major axis that the authors have found useful in orbit determination analysis have been presented in an attempt to raise awareness of this issue among the GPS community. It is hoped that this work will begin to stimulate innovations that will lead to better orbital GPS orbit determination performance.

ACKNOWLEDGEMENTS

Cary Semar of The Boeing Company Space and Defense Systems – Houston Division and the staff and support contractors of the Flight Design and Dynamics Division of NASA Johnson Space Center provided much of the data from Shuttle flights of the Honeywell EGI and SIGI and the Litton EGI. Lou Zyla of The Boeing Company Space and Defense Systems – Houston Division provided the data from the STS-51 Shuttle GPS experiment.

REFERENCES

1. R. Bate, D. Mueller, and J. White, *Fundamentals of Astrodynamics*, Dover, New York, 1971.
2. W. Lear, "Orbital Elements Including the J_2 Harmonic," Report No. 86-FM-18/JSC-22213, Rev. 1, Mission Planning and Analysis Division, NASA Johnson Space Center, 9/87.
3. Y. Park, et al., "Flight Test Results from Realtime Relative GPS Flight Experiment on STS-69," *Space Flight Mechanics 1995.*
4. C. Schroeder, B. Schutz, and P.A.M. Abusali, "STS-69 Relative Positioning GPS Experiment," *Space Flight Mechanics 1995.*
5. G. Moreau and H. Marcille, "FD1 Post-Flight Analysis and Evaluation Report," Matra Marconi Space France Report No. ARPK-RP-SYS-3744-MMT, 11/8/97.
6. E. Schiesser, et al. "Results of STS-80 Relative GPS Navigation Flight Experiment," *Space Flight Mechanics 1998.*
7. M. Lisano and R. Carpenter, "High-Accuracy Space Shuttle Reference Trajectories for the STS-77 GPS Attitude and Navigation Experiment (GANE)," *Space Flight Mechanics 1997.*